

Effects of confinement and surface enhancement on superconductivity

Emma Montecchi and Joseph O. Indekeu

Laboratorium voor Vaste-Stoffysica en Magnetisme, Katholieke Universiteit Leuven, B-3001 Leuven, Belgium

(Received 23 June 2000)

Within the Ginzburg-Landau approach a theoretical study is performed on the effects of confinement on the transition to superconductivity for type-I and type-II materials with surface enhancement. The superconducting order parameter is characterized by a negative surface extrapolation length b . This leads to an increase of the critical field H_{c3} and to a surface critical temperature in zero field T_{cs} , which exceeds the bulk T_c . When the sample is *mesoscopic* of linear size L the surface induces superconductivity in the interior for $T < T_c(L)$, with $T_c(L) > T_{cs}$. In analogy with adsorbed fluids, superconductivity in thin films of type-I materials is akin to capillary condensation and competes with the interface delocalization or “wetting” transition. The finite-size scaling properties of capillary condensation in superconductors are scrutinized in the limit that the ratio of magnetic penetration depth to superconducting coherence length $\kappa \equiv \lambda/\xi$ goes to zero, using analytic calculations. While standard finite-size scaling holds for the transition in nonzero magnetic field H , an anomalous critical-point shift is found for $H=0$. The increase of T_c for $H=0$ is calculated for mesoscopic films, cylindrical wires, and spherical grains of type-I and type-II materials. Surface curvature is shown to induce a significant increase of T_c , characterized by a shift $T_c(R) - T_c(\infty)$ inversely proportional to the radius R .

I. INTRODUCTION

The Ginzburg-Landau (GL) theory of superconductivity continues to deliver surprises.¹ In this paper we focus on some remarkable consequences of special boundary conditions that enhance superconductivity at the surface of the material. In fact, superconductivity is already known to be enhanced for the common situation of surfaces against vacuum or insulators, as was demonstrated by the discovery of the surface critical field H_{c3} .² We consider, however, different surfaces that enhance superconductivity more strongly. Within GL theory this is embodied phenomenologically by taking the surface extrapolation length b to be negative. It was shown that this not only leads to a further increase of the surface critical field H_{c3} ,³ but also to an increase of the surface critical temperature in zero field T_{cs} .⁴ The simple relation $\xi(T_{cs}) = -b$, with $\xi(T)$ the superconducting coherence length in bulk and in zero field, governs the shift from T_c to T_{cs} . Furthermore, for $b < 0$ interface delocalization transitions, which are the precise analogs of wetting transitions in adsorbed fluids, have been predicted for type-I superconductors.⁵

For a semi-infinite system with a planar surface the GL surface free energy functional, including the boundary contribution, reads

$$\begin{aligned} \gamma[\psi, \vec{A}] = & \frac{\hbar^2}{2mb} |\psi(0)|^2 + \int_0^\infty dx \left[\alpha |\psi|^2 + \frac{\beta}{2} |\psi|^4 \right. \\ & \left. + \frac{1}{2m} \left| \left(\frac{\hbar}{i} \vec{\nabla} - q\vec{A} \right) \psi \right|^2 + \frac{|\vec{\nabla} \times \vec{A} - \mu_0 \vec{H}|^2}{2\mu_0} \right]. \end{aligned} \quad (1.1)$$

The magnetic field is taken parallel to the surface. For this orientation the interface delocalization or wetting transition can occur, provided $\kappa \equiv \lambda/\xi < 1/\sqrt{2}$ (type-I superconductors)

and $b < 0$. Here, λ is the magnetic penetration depth and ξ is the zero-field superconducting coherence length. For $\kappa < 0.374$ the wetting transition is of first order, and is accompanied by a prewetting line that extends into the bulk normal phase in the H - T phase diagram, and terminates in zero field at T_{cs} .⁵ An experimental realization of the prewetting phenomenon is, in hindsight, provided by the twinning-plane superconductivity transition in Sn.⁴ The wetting transition itself has so far not been verified experimentally. For $\kappa > 0.374$ the wetting transition is predicted to be critical, without a prewetting line.⁵

In this paper we study the effect of confinement on the wetting phase diagram, and, in particular, we examine the increase of T_c . The situation we consider is analogous to that of a fluid adsorbed between parallel walls, which undergoes capillary condensation.⁶ This phenomenon occurs slightly below the saturated vapor pressure, and arises from a competition between surface contributions to the free energy, proportional to the surface area, and volume contributions, proportional to area times wall separation L . For large L , the pressure or chemical potential for which the fluid condenses between the walls, is shifted by a small amount, proportional to $1/L$, from the usual bulk coexistence line. In the presence of a wetting transition for the semi-infinite system, there is an interesting interplay between capillary condensation and prewetting, leading to surface triple points. We study the counterparts of these phenomena for type-I superconductors, in the low- κ limit.

In zero field, the increase of the surface critical temperature T_{cs} for samples with $b < 0$ is not limited to type-I materials, but occurs for type-I and type-II alike. It is therefore justified to devote special attention to the effect of confinement on this phenomenon. The increase of T_c is unique to superconductivity, since in fluids confinement generally suppresses the critical point of phase separation. In contrast, we find that in superconductors the critical temperature of a mesoscopic sample with surface enhancement not only exceeds

the bulk T_c , but is also greater than T_{c5} . We study this effect for planar films, cylindrical wires and spherical grains. For surfaces with curvature an important additional increase of T_c is found.

The assumption $b < 0$ is crucial here, since for $b = \infty$ (surfaces against vacuum or insulators) and *a fortiori* for $b > 0$ (surfaces against normal metals or ferromagnets) there is no increase of T_c relative to the bulk value. For $b = \infty$ the effect of confinement leads to a well-documented increase of the critical field and the presence of a tricritical point where the transition to superconductivity changes from second order to first order as the field is increased. The effects of sample topology for this case ($b = \infty$) have been the subject of thorough experimental⁷ and theoretical⁸ investigation.

This paper is organized as follows. In Sec. II we study the effect of confinement on the wetting phase diagram. The limit of strongly type-I superconductors turns out to be very instructive here, since various analytic results can be obtained for $\kappa \rightarrow 0$, the details of which are outlined in Sec. III. The finite-size scaling properties of the capillary condensation transition in nonzero field, and the link to the anomalous critical-point shift in zero field are addressed here. In Sec. IV we derive and discuss the increase of T_c for mesoscopic surface-enhanced superconductors. Conclusions and remarks pertaining to the experimental relevance of our results are presented in Sec. V.

II. CAPILLARY CONDENSATION AND PREWETTING FOR STRONGLY TYPE-I SUPERCONDUCTORS

In this section we discuss the precise analogy between the capillary condensation transition in a fluid confined between parallel walls and the transition to superconductivity of a mesoscopic film of type-I material in a parallel magnetic field. The surfaces of the film are characterized by surface enhancement of superconductivity (negative extrapolation length b) and we consider the case of identical surfaces, which is sufficient to address the basic phenomena. For temperatures sufficiently close to T_c , interface delocalization comes into play and allows us to study, in close analogy to what may happen in a confined fluid, how capillary condensation competes with the prewetting phenomenon.

There are four relevant lengths in our system: the magnetic penetration depth λ , the coherence length ξ , the surface extrapolation length b , and the film thickness L . In order to study the interplay between capillary condensation and prewetting most clearly and accurately, it is very useful to take the limit $\kappa \equiv \lambda/\xi \rightarrow 0$, corresponding to extreme type-I superconductors. It is important to specify that in taking this limit, we let λ tend to zero, while keeping the other three lengths finite. In this limit not only is the wetting transition of first order but also the prewetting transition remains of first order down to zero magnetic field, so that the competition with the capillary condensation transition (also of first order) is not complicated by second-order nucleation phenomena that occur for $\kappa > 0$. Furthermore, the vortex phase, which we find to play a role even for κ considerably less than $1/\sqrt{2}$ in a film with enhanced surfaces, is unimportant at $\kappa = 0$.

In addition to these reasons pertaining to clarity, the limit $\kappa \rightarrow 0$ offers the major advantage that the problem can be

studied analytically, and the important finite-size scaling laws for the phase transitions can be calculated exactly (see next section for details). Several of these laws continue to hold, in as far as the leading singularity in the asymptotic regime of thick films is concerned, for small $\kappa > 0$, as long as the phase diagram undergoes quantitative changes only. Therefore, many of the properties that we can demonstrate analytically at $\kappa = 0$, serve as a good first approximation for a significant part of the type-I regime. We have verified this by numerical computations for $\kappa > 0$.

The usefulness of taking the zero- κ limit has already become clear in previous studies of interfacial properties in type-I superconductors, most notably in the derivation of an exact interface potential for wetting and prewetting.⁹ Moreover, it has been shown extensively that the thermodynamic behavior at $\kappa > 0$ (but not exceeding $1/\sqrt{2}$) can often be captured by means of rapidly converging expansions in the parameter κ .^{10,11}

The two basic physical states of the film consist of either superconducting surface sheaths, extending from one or both surfaces into the interior, or a superconducting film state, which occupies the whole space between the surfaces. The former correspond to prewetting layers and the latter to capillary condensation. For computing these states we recall that for $\kappa = 0$ the magnetic induction $\dot{A}(x)$ and the superconducting wave function $\psi(x)$ exclude one another in space.⁹ Furthermore, since \dot{A} is a simple step function, the only pertinent GL equation is that for ψ , which after suitable rescaling (as in Ref. 9) reads

$$\dot{\psi} = \pm \psi + \psi^3. \quad (2.1)$$

The $+$ ($-$) signs pertain to $T > T_c$ ($T < T_c$), respectively. Note that, with the present rescaling convention, lengths are measured in units of the (zero-field) coherence length ξ , and in the bulk superconducting phase, $\psi = 1$.

The boundary conditions are

$$\dot{\psi}(0) = \xi \psi(0)/b, \quad (2.2)$$

$$\dot{\psi}(L/\xi) = -\xi \psi(L/\xi)/b.$$

The useful first integral of Eq. (2.1),

$$\dot{\psi}^2 = \pm \psi^2 + \psi^4/2 + C \quad (2.3)$$

allows one to employ a simple phase-portrait analysis for determining the characteristics of all possible solutions. The integration constant C is determined using the boundary conditions. For $T < T_c$ capillary condensation states exist for $C < 1/2$, while for $T > T_c$ they occur for $C < 0$. They are symmetric with respect to the middle plane of the film, $\psi(x) = \psi(L/\xi - x)$. For these states $\psi(x)$ has the shape of a ‘‘hammock,’’ with a minimum at $x = L/2\xi$. C is a smooth function of L which tends to $1/2$ for large L , as $\psi(L/2\xi)$ tends to the bulk value 1. An interesting point to note is that the magnetic field H is fully expelled in these states and therefore the profiles $\psi(x)$ do not depend on H . In particular, $C(L)$ is independent of H .

In contrast, the prewetting states depend on the applied field. These states are characterized by profiles $\psi(x)$, interrupted by a magnetic ‘‘gap’’ in which $\psi(x) = 0$. The phase

portrait analysis indicates that two types of solutions can be considered: symmetric states consisting of two superconducting surface sheaths located on $x \in [0, l/\xi]$ and $[(L-l)/\xi, L/\xi]$, with a central gap separating them, or asymmetric states with a sheath at one surface only, on $x \in [0, l/\xi]$, followed by a gap extending to the other surface. In practice the asymmetric states are irrelevant, even for $l > L/2$, since their free energy is higher than that of symmetric states (either of prewetting type, with a central gap, or of capillary condensation type, without a gap). For prewetting states, C depends on H and not on L . Its form $C(H_R) = H_R^2$ is the same as for the semi-infinite system, since the ‘‘gap’’ acts in the same way as a normal phase (N) in bulk. The quantity H_R is a reduced field defined in Ref. 9 and related to H in the manner $H_R \propto \xi^2 H$. The value of H_R^2 determines the magnitude (squared) of the gradient of ψ at the interior points $x = l/\xi$ and $x = (L-l)/\xi$ at which ψ vanishes. For $T < T_c$, at bulk two-phase (SC/N) coexistence, $C = 1/2$, while in the bulk normal phase, $C > 1/2$. The term ‘‘bulk’’ refers to an infinite system (without surfaces, in principle).

We can conveniently express the film thickness using the profile of a capillary condensed state (‘‘cap’’), through the relation

$$L = 2\xi \int_{\psi_m}^{\psi_{\text{cap}}(0)} d\psi (\pm \psi^2 + \psi^4/2 + C)^{-1/2}. \quad (2.4)$$

Here, $\psi_m \equiv \psi(L/2\xi)$, the value in the middle of the film. Likewise, we can obtain the thickness of a surface sheath in the prewetting (PW) state through

$$l = \xi \int_0^{\psi_{\text{PW}}(0)} d\psi (\pm \psi^2 + \psi^4/2 + H_R^2)^{-1/2}. \quad (2.5)$$

For explicit expressions for ψ_m , $\psi_{\text{cap}}(0)$, and $\psi_{\text{PW}}(0)$, see the Appendix.

Similar compact expressions are available for the reduced (i.e., dimensionless) free energies. For capillary condensed states

$$\gamma_{\text{cap}} = 2 \int_{\psi_m}^{\psi_{\text{cap}}(0)} d\psi (H_R^2 - \psi^4/2) (\pm \psi^2 + \psi^4/2 + C)^{-1/2}. \quad (2.6)$$

Using Eq. (2.4) this can be simplified by separating out the dependence on the magnetic field, which is just $H_R^2 L/\xi$, the free energy cost of expelling the field over the whole thickness of the film.

For prewetting states the free energy of a symmetric state with two surface sheaths is

$$\gamma_{\text{PW}} = 2 \int_0^{\psi_{\text{PW}}(0)} d\psi (H_R^2 - \psi^4/2) (\pm \psi^2 + \psi^4/2 + H_R^2)^{-1/2}. \quad (2.7)$$

In order to be able to discuss the phase diagram for temperatures below, above, and at bulk T_c , it is convenient to express the thickness of the film in units of $|b|$ instead of ξ (since ξ diverges at T_c in zero field). It is understood that the value of b is the result of the surface preparation of the sample, and can therefore be considered a material constant within the explored ranges of field and temperature.

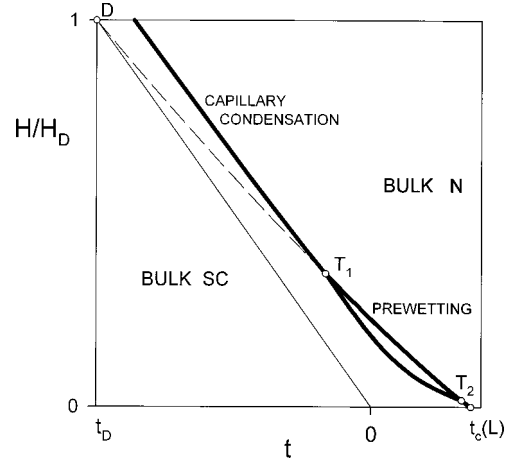


FIG. 1. Capillary condensation phase diagram for strongly type-I superconductors with surface enhancement, for a film of thickness $L/|b|=8$, in units of the surface extrapolation length b ($b < 0$). The magnetic field H is scaled with the field H_D at the interface delocalization transition D . The temperature variable is $t \equiv (T - T_c)/(T_{cs} - T_c)$. The capillary condensation transition runs mostly parallel to the bulk coexistence line. It meets the prewetting transition at a film triple point $T1$, and again at $T2$. It terminates at the film critical point in zero field, at $T_c(L) > T_{cs}$, but very close to T_{cs} (imperceptible difference). The solid lines indicate first-order phase transitions for the film. The dashed line is the (metastable) continuation of the prewetting line.

In order to show most clearly the topology of the new phase diagram of the thin film with surface enhancement, we have chosen the (reduced) thickness $L/|b|=8$. The result is presented in Fig. 1. The temperature variable is $t \equiv (T - T_c)/(T_{cs} - T_c)$, so that the first-order interface delocalization transition, or ‘‘wetting’’ transition, is located at $t_D < 0$, while the bulk critical point in zero field is at $t_c = 0$ and the surface critical point in zero field is at $t_{cs} = 1$. The magnetic field H is in units of H_D , the wetting transition field. The ratio H/H_D is related to H_R through the equation $H/H_D = \sqrt{2} H_R (\xi/b)_D^2 / (\xi/b)^2$. The thin straight line from D to the origin is the bulk two-phase coexistence line. The new phase transitions relevant to the mesoscopic film are indicated by thick solid lines.

The main transition is the capillary condensation line, which consists of three parts. For high fields this line is more or less parallel to the bulk reference line, and represents a transition from a fully normal film to a fully superconducting film. Between $T1$ and $T2$, however, for decreasing H , capillary condensation is preceded by the prewetting transition. The film thus goes superconducting in two distinct steps: (i) from a fully normal state to a state with two superconducting surface sheaths and a normal gap and (ii) from the latter to a fully superconducting film. At transition (ii) the gap between the surface sheaths is still finite. Incidentally, we can compute the line in the phase diagram on which $l = L/2$, so that the gap vanishes and the two surface sheaths touch one another. For all temperatures between the wetting point and the prewetting critical point, this line lies at lower fields than the capillary condensation transition, and consequently has no physical significance. Finally, for temperatures between that of $T2$ and $t_c(L)$, the transition proceeds in a single step, from fully normal to fully superconducting.

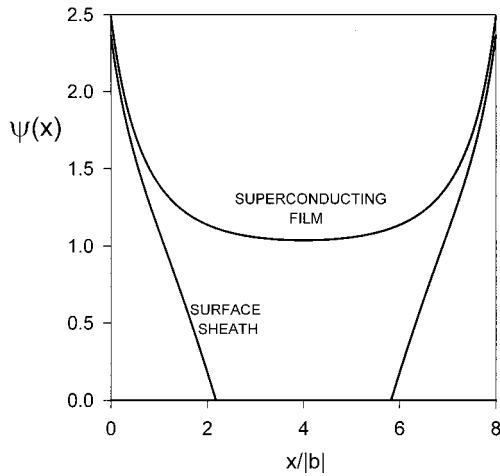


FIG. 2. Three coexisting film phases at triple point $T1$ of Fig. 1. A normal phase ($\psi=0$) coexists with a surface superconducting film (with two sheaths), and with a capillary condensed superconducting film.

The prewetting phenomenon is thus confined to an “island” in the phase diagram, where a film with superconducting surface layers and a normal interior is thermodynamically stable. All transitions in nonzero field are of first order. The points $T1$ and $T2$ are genuine triple points of the film. The three coexisting film phases are represented by their wave function profiles in Fig. 2. Likewise, Fig. 3 illustrates the triple point $T2$. The prewetting line (between $T1$ and $T2$) lies exactly on the prewetting line of the semi-infinite system (dashed line), which extends from the wetting point D to the surface critical point of the semi-infinite system in zero field, at $t=t_{cs}=1$.

In zero field the capillary condensation ends in a critical point, at $t=t_c(L)$. This critical point will be discussed in detail in Sec. V. We shall derive there that $t_c(L)$ is only slightly above t_{cs} . On the scale of the figure the two points appear coincident.

Upon lowering $L/|b|$ the points $T1$ and $T2$ approach each other, and for $L/|b|$ between 6 and 7 the prewetting “island” vanishes. For $L/|b|<6$ only the capillary condensation tran-

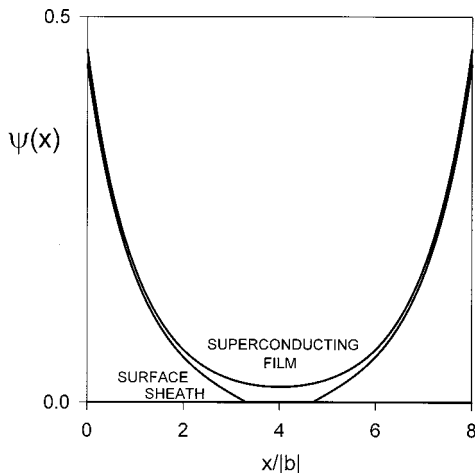


FIG. 3. Three coexisting film phases at triple point $T2$ of Fig. 1. Under these conditions the sample in bulk would show no superconductivity at all.

sition remains. For example, for $L/|b|=1$ the capillary condensation line appears as a straight line parallel to the bulk coexistence line, and ends in zero field at $t_c \approx 2.4$ (see Sec. IV).

On the other hand, upon increasing $L/|b|$ the triple point $T2$ moves rapidly to zero field and $t=t_{cs}$, and $T1$ moves slowly towards the wetting point D . The prewetting line remains fixed. The capillary condensation transition converges, for $T<T_c$, to the bulk coexistence line. However, for $T>T_c$, the capillary condensation line converges to the segment $[T_c, T_{cs}]$ of the temperature axis (at $H=0$). This is a consequence of the anomalous critical-point shift in zero field. The phase boundary thus develops a *corner* singularity at the origin ($t=0, H=0$). The precise manner in which the phase boundary scales in the limit $L \rightarrow \infty$ is the subject of the next section.

III. FINITE-SIZE SCALING OF CAPILLARY CONDENSATION

In order to examine how the capillary condensation phase boundary approaches the bulk coexistence line in the limit $L \rightarrow \infty$ we distinguish the following regimes.

A. $T<T_D$: below the wetting transition, approaching partial wetting

In this regime the complication of surface superconductivity does not arise and the transition is from the normal phase directly to a superconducting film with complete expulsion of the magnetic field. The transition occurs when the free energy γ_{cap} , given in Eq. (2.6), equals that of the normal phase, which is zero. For large L this condition is very well approximated by replacing the upper and lower limits of the integral by their asymptotic values $\psi_{cap}(0) \rightarrow \psi(0)$ and $\psi_m \rightarrow 1$. Here, $\psi(0)$ is the surface value of the wave function profile associated with the superconducting phase in bulk, at temperature T . This leads to the familiar result, akin to Laplace’s or Kelvin’s equation for a confined fluid,⁶ expressing the free energy balance between a cost in bulk and a cost in surface contributions

$$(H_R^2 - 1/2)L/\xi = -2\gamma_{W,SC}. \quad (3.1)$$

The right-hand side (rhs) is by definition $-\lim_{L \rightarrow \infty} \gamma_{cap}$ and represents (minus) the surface free energy of two wall/SC “interfaces.” Since $\gamma_{W,N}=0$, in the absence of superconducting surface sheaths, the rhs actually equals $2\gamma_{SC/N} \cos \theta$, familiar in the context of Young’s equation for the contact angle θ in the partial wetting regime. The left-hand side (lhs) gives the net free energy cost, per unit volume, of expelling the magnetic field (cost H_R^2) and, simultaneously, going superconducting (gain $1/2$), multiplied by the thickness of the film. This net cost is positive for fields higher than the coexistence field (commonly referred to as critical field of the superconductor) $H_{R,c} = 1/\sqrt{2}$. Equation (3.1) predicts that the capillary transition field $H_R(L)$ approaches the coexistence field $H_{R,c}$ according to the power law

$$[H_R(L) - H_{R,c}] \sim \sqrt{2} \xi \frac{|\gamma_{w,SC}|}{L}. \quad (3.2)$$

The exponent of L , -1 , simply reflects the difference between the surface dimension $d-1$ and the bulk dimension d .

Numerical computations show that Eq. (3.1) is extremely accurate, even for thin films. For example, for ‘‘temperature’’ $\xi/b = -0.5$, Eq. (3.1) is satisfied to an accuracy of 0.1% already for $L/|b|=2$. The deviation for $L/|b|=1$ is about 3%. Therefore, for practical purposes, Eq. (3.1) is correct for $L/|b| \geq 2$. The wetting transition (D) occurs at $\xi/b = (\xi/b)_D \approx -0.60$, and for temperatures $T_D < T < T_c$ Eq. (3.1) must be modified as follows.

B. $T_D < T < T_c$: the prewetting regime, approaching complete wetting

In this regime the capillary condensation competes with the prewetting transition. To a first approximation the surface free energy balance takes the Laplace or Kelvin form, analogous to Eq. (3.1),

$$(H_R^2 - 1/2)L/\xi = 2(\gamma_{w,N} - \gamma_{w,SC}) = 2\gamma_{SC,N}, \quad (3.3)$$

where $\gamma_{w,N}$ is the surface free energy of a semi-infinite system with a macroscopic surface superconducting layer (complete wetting). The last equality expresses that Antonov’s rule holds for complete wetting.¹²

However, this approximation is too crude. It neglects first of all that L should be replaced by $L-2l$ to take into account the thickness of the prewetting layers, constituting the part of the film which is already superconducting before capillary condensation occurs. But even with this correction, the resulting approximation is still not satisfactory, in comparison with numerical computations. In what follows we derive an accurate analytic approximation for large L .

We start from the exact condition for capillary condensation

$$\gamma_{PW} = \gamma_{cap}. \quad (3.4)$$

The magnetic field terms in these free energies lead to contributions $2H_R^2 l/\xi$ and $H_R^2 L/\xi$, respectively, as is seen from the set of equations (2.4)–(2.7). In the limit $L \rightarrow \infty$, the capillary condensation field H_R approaches the bulk coexistence field $H_{R,c} = 1/\sqrt{2}$, and the prewetting layer thickness l diverges, but very slowly. To see this in detail, we work out the integral and obtain the magnetic-field dependence of l ,

$$l(H_R)/\xi = \frac{1}{\sqrt{2}} \ln \frac{1}{H_R^2 - 1/2} + l_1/\xi + o(1). \quad (3.5)$$

The divergence is only logarithmic, so that the constant l_1/ξ is an important correction for numerical purposes. Furthermore, it is the only important correction, since we verified that the remainder is insignificant, up until $H_R^2 - 1/2 = \mathcal{O}(1)$. We remark that the upper spinodal of the prewetting transition occurs at $H_R^2 = [1 + (\xi/b)^2]^2/2$. The remainder is indicated by $o(1)$, which signifies that it goes to zero as $H_R^2 \rightarrow 1/2$. Numerically these terms are found to vanish as $H_R^2 - 1/2$, or $(H_R^2 - 1/2) \ln[1/(H_R^2 - 1/2)]$.

The constant l_1/ξ can be calculated analytically, with the result

$$l_1/\xi = \sqrt{2} \ln 2 + \frac{1}{\sqrt{2}} \ln \frac{\psi(0) - 1}{\psi(0) + 1} + 2 \int_0^\infty du (2u^2 + 1)^{-1/2} - 2 \int_1^\infty du (2u^2)^{-1/2}. \quad (3.6)$$

The value of $\psi(0)$ here corresponds to the limit of bulk two-phase coexistence, and is determined through $\psi(0)^2 = 1 + (\xi/b)^2 + \{[1 + (\xi/b)^2]^2 - 1\}^{1/2}$. Typical values of l_1/ξ are of order 1, confirming the importance of this constant next to the leading logarithm in Eq. (3.5). For example, for $\xi/b = -1$, $l_1/\xi \approx 1.640$.

The geometrical interpretation of l_1/ξ is straightforward. Keeping only the leading and next-to-leading terms in $l(H_R)/\xi$ we arrive at the identification

$$l_1/\xi \approx l(H_{R,1})/\xi, \quad (3.7)$$

with $H_{R,1}^2 - 1/2 \equiv 1$. This is qualitatively correct. For example, for ‘‘temperature’’ $\xi/b = -1$, $l_1/\xi = 1.640$ while $l(H_{R,1})/\xi = 1.504$. Thus, l_1/ξ corresponds essentially to the thickness of a *thin* surface sheath at a magnetic field well above the critical field. This thickness (in units of ξ) is of order 1. Consequently, the leading logarithm in Eq. (3.5) gives the intrinsic or ‘‘net’’ thickness of the wetting layer which develops close to bulk coexistence.

Having established the slow divergence of l , and contrasting it with the more rapid divergence of L , which is essentially proportional to $1/(H_R^2 - 1/2)$, we collect carefully all terms proportional to $H_R^2 - 1/2$ in Eq. (3.4) and find

$$(H_R^2 - 1/2)(L - 2l)/\xi = 2\gamma_{SC,N} + (H_R^2 - 1/2)[\sqrt{2} + o(1)] + \mathcal{O}(e^{-\sqrt{2}L/\xi}), \quad (3.8)$$

where $o(1)$ vanishes for $H_R^2 \rightarrow 1/2$. A summary of the derivation is given in the Appendix. The lhs features the net cost of expelling the magnetic field, while the first term on the rhs gives the cost of having two SC/N interfaces. Especially interesting, and calculable analytically, is the correction to the surface tension $(H_R^2 - 1/2)\sqrt{2}$, appearing as the second term in the rhs. Precisely in view of the slow divergence of l this contribution is numerically significant in combination with the lhs. Taking it into account greatly improves the accuracy of the approximation.

The surface tension correction has an interesting physical interpretation. In the complete wetting regime at bulk two-phase coexistence a superconducting/normal (SC/N) interface *constrained* at a distance l from the surface has a free energy (per unit area) that is higher than that of an *equilibrium* interface (infinitely) far away from the surface, by an amount which is given by the so-called interface potential $V(l)$. This excess free energy is known exactly in the $\kappa=0$ limit,⁹ and we are concerned here with the tail of $V(l)$ for large l , given by $V(l) \propto \exp(-\sqrt{2}l/\xi)$. Therefore, the free energy cost of a constrained interface is easily found, by inserting the logarithmic divergence (3.5), to be proportional to $H_R^2 - 1/2$. Thus we arrive at the interpretation that the surface tension correction is due to the interaction or ‘‘interfer-

ence” of the interface with the surface, which in the broader context of confined interfaces is often referred to as entropic repulsion.¹³

In the same spirit, a correction is present for the capillary condensed superconducting state, relative to a superconducting state with infinite surface separation L . This correction is due to the interaction between the surfaces bounding the film, and also decays exponentially with separation. However, since the distance is now L instead of l , this contribution is of order $\exp(-\sqrt{2}L/\xi)$, which is negligible for our purposes (see the Appendix for details).

In conclusion, in the complete wetting regime the finite-size shift of the transition to superconductivity has the same asymptotic scaling behavior $H_R - H_{R,c} \propto 1/L$ as in the partial wetting regime, but quantitatively L must be shortened by twice the wetting layer thickness l , and an effective further correction $\sqrt{2}\xi$ must be subtracted from L in order to take into account the distortion of the two constrained SC/N interfaces.

C. $T=T_c$: the bulk critical isotherm

The finite-size scaling properties of the transition to film superconductivity at T_c are interesting and merit a separate study, since they invoke *universal* quantities associated with the bulk critical point. At $T=T_c$ the zero-field coherence length is infinite, and we cannot use it as the unit of length. Instead we use $|b|$. The wave function must also be rescaled, because the normalization $\psi_{\text{bulk}}=1$ is inconvenient at T_c . Simple universal GL equations result when we rescale $x \rightarrow (\xi/|b|x)$, $\psi \rightarrow (\xi/|b|)\psi \equiv \phi$, $H_R \rightarrow (\xi/b)^2 H_R \equiv h_R$. The ratio H/H_D is invariant and equals $\sqrt{2}h_R(\xi/b)_D^2$.

The GL equation now reads

$$\dot{\phi} = \phi^3 \quad (3.9)$$

and the boundary conditions take the form

$$\dot{\phi}(0) = -\phi(0), \quad (3.10)$$

$$\dot{\phi}(L/|b|) = \phi(L/|b|).$$

Writing the first integral of Eq. (3.9) as

$$\dot{\phi}^2 = \phi^4/2 + c \quad (3.11)$$

we obtain for the film thickness,

$$L = 2|b| \int_{\phi_m}^{\phi_{\text{cap}}(0)} d\phi (\phi^4/2 + c)^{-1/2}, \quad (3.12)$$

with $\phi_m = (-2c)^{1/4}$ and $\phi_{\text{cap}}(0)^2 = 1 + (1 - 2c)^{1/2}$. For $L \rightarrow \infty$, c approaches zero from below and ϕ_m vanishes. For the thickness of the superconducting surface sheath we have

$$l = |b| \int_0^{\phi_{\text{PW}}(0)} d\phi (\phi^4/2 + h_R^2)^{-1/2}, \quad (3.13)$$

with $\phi_{\text{PW}}(0)^2 = 1 + (1 - 2h_R^2)^{1/2}$.

We remark that, although $T=T_c$ marks the terminus of bulk two-phase coexistence, two-phase coexistence for the mesoscopic film continues to exist. Therefore, we will con-

tinue to use the terminology “capillary condensation” and “prewetting” in the same sense as in the previous subsections.

Before discussing the free energies we examine how l behaves when the field h is turned to zero. A simple rescaling in Eq. (3.13) suffices to extract the leading term

$$l/|b| \approx h_R^{-1/2} \int_0^\infty dx (1 + x^4/2)^{-1/2} \approx 2.20488 h_R^{-1/2}. \quad (3.14)$$

This power-law divergence is much faster than the logarithmic behavior found in the prewetting regime below T_c , approaching bulk two-phase coexistence. Experimentally, this implies that the diamagnetic response due to the surface superconducting sheath may be easier to detect when lowering H at $T=T_c$ than at $T < T_c$.

A similar reasoning leads to a simple relation between L and c , in the thick film limit

$$L/|b| \approx (-c)^{-1/4} 2^{5/4} \int_1^\infty dx (x^4 - 1)^{-1/2}. \quad (3.15)$$

The integral equals 1.31103. So we conclude that $c(L)$ decays as a power law, in contrast with the exponential decay seen in the Appendix, Eq. (A12).

We now turn to the free energies. For capillary condensed states at bulk T_c ,

$$\gamma_{\text{cap}} = 2 \int_{\phi_m}^{\phi_{\text{cap}}(0)} d\phi (h_R^2 - \phi^4/2) (\phi^4/2 + c)^{-1/2}, \quad (3.16)$$

while for prewetting states,

$$\gamma_{\text{PW}} = 2 \int_0^{\phi_{\text{PW}}(0)} d\phi (h_R^2 - \phi^4/2) (\phi^4/2 + h_R^2)^{-1/2}. \quad (3.17)$$

Working out the condition $\gamma_{\text{PW}} = \gamma_{\text{cap}}$ for capillary condensation we find

$$h_R^2(L - 2l)/|b| = \delta\gamma_{\text{PW}} - \delta\gamma_{\text{cap}}. \quad (3.18)$$

Using Eq. (3.14) we see that the second term in the lhs is of order $h_R^{3/2}$. The first term on the rhs is the surface free energy cost of *constraining* a surface sheath at $H=0$ and $T=T_c$ to terminate at $x=l/|b|$ instead of assuming its equilibrium power-law decay $\phi(x) \propto 1/x$. This power-law decay is the analog of “critical adsorption” for fluids.¹⁴ Analytic calculation gives

$$\delta\gamma_{\text{PW}} = h_R^{3/2} \sqrt{2} \int_0^\infty dx x^2 [1 - (1 + 2/x^4)^{-1/2}]. \quad (3.19)$$

The integral equals 1.03939. The constrained surface sheath can be interpreted as a constrained interface interacting with the surface. This interpretation is quite unconventional in this case, since an equilibrium interface does not exist at bulk T_c . Nevertheless, assuming the existence of an interface potential $V(l)$ for the constrained interface leads us to infer $V(l) \propto l^{-3}$, in view of Eqs. (3.14) and (3.19). The exponent -3 is reminiscent of finite-size interactions at bulk criticality and will show up again in the next paragraph. Incidentally,

note that $\delta\gamma_{\text{PW}} > 0$, corresponding to repulsion between the surface and the constrained interface (“unlike” surfaces repel).

The second correction $\delta\gamma_{\text{cap}}$ is the finite-size interference free energy between the two surfaces at separation L bounding the film, in the superconducting state at bulk T_c and in zero field. This interference is akin to the generalized Casimir effect.^{15,16} Analytic calculation gives

$$\delta\gamma_{\text{cap}} = -2^{5/4}(-c)^{3/4} \left(\int_1^\infty d\phi \phi^2 (1 - 1/\phi^4)^{-1/2} - \int_0^\infty d\phi \phi^2 \right). \quad (3.20)$$

The integrals add up to 0.43701. Converting the $|c|$ -dependence into an L dependence, using Eq. (3.15) we observe that the finite-size interaction is attractive (“like” surfaces attract) and decays in the manner L^{-3} . We scrutinize this generalized Casimir effect for superconductors and the associated universal exponents and amplitudes elsewhere.¹⁷

Returning now to Eq. (3.18) we see by simple inspection that $h_R \propto L^{-2}$, and that all the leading corrections we extracted are of the same order L^{-3} . We are therefore left with the simple problem of solving for the amplitude A in the asymptotic behavior

$$h_R \approx A(L/|b|)^{-2}. \quad (3.21)$$

Numerical solution gives $A \approx 36.2869$. The fact that the exponent of L equals -2 is linked to the fact that the mean-field value of the critical exponent ν_H is $1/2$. This exponent describes the divergence of the field-dependent coherence length $\xi(h_R)$ along the bulk critical isotherm approaching the bulk critical point

$$\xi(h_R) \propto h_R^{-\nu_H}. \quad (3.22)$$

The transition to superconductivity for the film occurs when $\xi(h_R) \approx L$, whence Eq. (3.21). The sense in which *universality* holds is governed here by the validity of mean-field theory for classical superconductors.

A numerical computation of the finite-size shift of the critical field at bulk T_c supports the analytic leading result (3.21) and suggests that the next-to-leading term is of order $(L/|b|)^{-3}$, implying slow convergence. For $L/|b|=10$ the correction to the leading term is about 31%, while at $L/|b|=100$ the correction is about 3.7%.

D. $T_c < T < T_c(L)$: the bulk supercritical region

Even though $T > T_c$, in this regime we still find a competition between prewettinglike states and capillary condensation. The main difference with respect to the prewetting region below T_c is that an equilibrium SC/N interface and hence also its surface tension no longer exist. Therefore, the main modification to Eq. (3.8) is that the first term on the rhs is absent for $T > T_c$. Furthermore, since the critical field is zero, the combination $H_R^2 - 1/2$ simplifies to H_R^2 . The other modifications to Eq. (3.8) will now be studied in detail.

We start, as usual, from Eq. (3.4). The magnetic field terms again lead to the net free energy contribution $H_R^2(L/\xi - 2l/\xi)$. The prewetting layer thickness l has a different interpretation than for $T < T_c$. Above T_c no thick wetting layer can develop, since the infinite system consists of a single normal phase only. So, l just measures the extent of penetration into the bulk of the *tail* of the surface superconducting sheath. As the field H goes to zero the superconducting wave function no longer vanishes at $x=l/\xi$ but decays exponentially as a function of the distance x from the surface, so that, mathematically, l diverges although physically the penetration is of short range only.

To see how l behaves above T_c , we employ Eq. (2.5) with the + sign. We obtain

$$l(H_R)/\xi = \ln \frac{1}{H_R} + l_2/\xi + o(1). \quad (3.23)$$

This is similar to Eq. (3.5). The constant l_2/ξ can be calculated analytically, with the result

$$l_2/\xi = \ln \frac{4\psi(0)}{1 + \sqrt{1 + \psi(0)^2/2}}. \quad (3.24)$$

The value of $\psi(0)$ here corresponds to the zero-field limit, and is determined through $\psi(0)^2 = 2[-1 + (\xi/b)^2]$. Typical values of l_2/ξ are of order 1. For example, for $\xi/b = -2$, $l_2/\xi \approx 1.184$. However, l_2/ξ approaches zero and changes sign as $\xi/|b|$ is decreased to about 1.07, not far from the surface critical point T_{cs} .

The geometrical interpretation of l_2/ξ is similar to that of l_1/ξ discussed previously for $T < T_c$. To a first approximation we can identify

$$l_2/\xi \approx l(H_{R,2})/\xi, \quad (3.25)$$

with $H_{R,2} = 1$. This is reasonable. For instance, for $\xi/b = -2$, $l_2/\xi = 1.184$ while $l(H_{R,2})/\xi = 1.381$. So we arrive at the interpretation that l_2/ξ corresponds to the thickness of a *thin* surface sheath in a finite field (of reduced strength unity). This interpretation can only be used as long as the (reduced) spinodal field exceeds 1. The spinodal line for prewetting states above T_c is determined by $H_R = [(\xi/b)^2 - 1]/\sqrt{2}$. Consequently, Eq. (3.25) makes sense as long as $\xi/|b| > 1.554$. The remainder $o(1)$ in Eq. (3.23) appears to vanish in the manner $H_R^2 \ln(1/H_R)$ as follows from numerical inspection.

We now return to the condition for capillary condensation, which can be written as

$$H_R^2(L - 2l)/\xi = \int_{\psi_m}^{\psi_{\text{cap}}(0)} d\psi \psi^4 (\psi^2 + \psi^4/2 + C)^{-1/2} - \int_0^{\psi_{\text{PW}}(0)} d\psi \psi^4 (\psi^2 + \psi^4/2 + H_R^2)^{-1/2} \quad (3.26)$$

with $\psi_m^2 = -1 + (1 - 2C)^{1/2}$, $\psi_{\text{cap}}(0)^2 = -1 + (\xi/b)^2 + \{-1 + (\xi/b)^2\}^2 - 2C\}^{1/2}$, and $\psi_{\text{PW}}(0)^2 = -1 + (\xi/b)^2 + \{-1 + (\xi/b)^2\}^2 - 2H_R^2\}^{1/2}$. The two integrals can be studied fairly easily, since expanding in the small parameters H_R^2

or $|C|$ poses no problems regarding the exchange of differentiation and integration, in contrast with the case $T < T_c$. We find analytically that the integrals are, in leading order, simply proportional to C and H_R^2 , respectively. The result is

$$H_R^2(L-2l)/\xi = H_R^2[1+o(1)] - C[1+o(1)], \quad (3.27)$$

where the two terms $o(1)$ vanish in the limits $H_R \rightarrow 0$ and $C \rightarrow 0$, respectively.

We are thus left with the final task of determining the dependence $C(L)$. This can also be done analytically, starting from Eq. (2.4). In the limit $C \rightarrow 0$, with $C < 0$, we readily find the leading behavior

$$L/\xi = \ln(-1/C) + L_2/\xi + o(1) \quad (3.28)$$

The constant is given by the expression

$$\frac{L_2}{\xi} = 2l_2/\xi, \quad (3.29)$$

with l_2/ξ as given in Eq. (3.24). This quantity varies smoothly between $-\infty$ for $\xi/b = -1$ (surface critical point T_{cs}) and the value $5 \ln 2 \approx 3.466$ for $\xi/b \rightarrow -\infty$ (bulk critical point T_c). It changes sign at ‘‘temperature’’ $\xi/b \approx -1.064$. The remainder $o(1)$ is numerically found to be proportional to $C \ln(-1/C)$.

Inverting Eq. (3.28) to get $C(L)$ we arrive at the following conclusion, which is the counterpart of Eq. (3.8) for temperatures above T_c ,

$$H_R^2(L-2l)/\xi = H_R^2[1+o(1)] + e^{L_2/\xi} e^{-L/\xi} \quad (3.30)$$

which implies an exponentially fast decrease of the field as a function of L or, equivalently, a logarithmic divergence of L as a function of $1/H_R$. This is in sharp contrast with the simple power law found for the usual capillary condensation below T_c .

Since now l and L behave essentially in the same manner (logarithmic) as a function of $1/H_R$, we investigate numerically the interesting difference $L-2l$, in the limit $H \rightarrow 0$. Using Eqs. (3.23), (3.28) and taking advantage of the equality (3.29), we find that the constants cancel and we are left with

$$(L-2l)/\xi \approx \ln(-H_R^2/C). \quad (3.31)$$

On the other hand, Eq. (3.30) implies

$$L/\xi - 2l/\xi - 1 \approx -C/H_R^2. \quad (3.32)$$

In combination with the previous result the difference $\Delta \equiv (L-2l)/\xi$ must solve the equation

$$\Delta = \ln \frac{1}{\Delta - 1}. \quad (3.33)$$

Numerically, this gives $\Delta \approx 1.2785$. In conclusion, the difference $L-2l$ converges to a *finite* length, as we follow the capillary condensation transition into the asymptotic regime $L \rightarrow \infty$. We have verified this analytic result numerically, and the agreement is very good for sufficiently large L . For instance, for $\xi/b = -1.5$, Δ is reproduced to 4 digits if we take $L/|b| = 20$. For $\xi/b = -2$ we achieve similar accuracy taking $L/|b| = 25$.

IV. CRITICAL-POINT SHIFT IN ZERO FIELD

In zero magnetic field the transition to superconductivity is of second order and can be calculated using the linearized GL equation. This can be seen by calculating, in the presence of a magnetic field, the location of the tricritical point where the order of the transition changes from second to first order, as the field is increased. Furthermore, in zero field the dependence on the GL parameter κ drops out so that the results are valid for all classical superconductors, regardless of their type. We study three different geometries: planar slab, cylindrical wire, and spherical grain. For each geometry we calculate the critical temperature as a function of the thickness (or diameter) of the mesoscopic system with surface enhancement of superconductivity.

A. Planar film

For the planar sample, a slab or film with two parallel surfaces, we allow in general a different enhancement on each surface. Thus we assume two surface extrapolation lengths b_1 and b_2 . Scaling all lengths with the zero-field coherence length ξ leads to the GL equation

$$\dot{\psi} = \pm \psi \quad (4.1)$$

with boundary conditions

$$\dot{\psi}(0) = (\xi/b_1)\psi(0),$$

$$\dot{\psi}(L/\xi) = -(\xi/b_2)\psi(L/\xi). \quad (4.2)$$

Since we are interested mostly in enhancing superconductivity ($b < 0$) we are concerned with $T \geq T_c$, corresponding to the $+$ sign in the rhs of Eq. (4.1).

Solving these equations leads to the following relation describing the onset or *nucleation* condition for superconductivity in the film

$$\left(\frac{1 + \xi/b_1}{1 - \xi/b_1} \right) \left(\frac{1 + \xi/b_2}{1 - \xi/b_2} \right) = e^{-2L/\xi}. \quad (4.3)$$

Considering the extrapolation lengths as material constants imposed by the sample preparation (mechanical surface treatment, physical surface deposition technique, or chemical modification such as oxidation, etc.) the temperature dependence is contained in the variable ξ . In order to obtain direct estimates of the finite-size shift of the film critical point, we focus on the following particular cases: similar surfaces and dissimilar surfaces.

Similar surfaces. In this case we assume, for simplicity, $b_1 = b_2 = b$ and $b < 0$. We can then work out Eq. (4.3) to obtain the critical film thickness $L/|b|$ as a function of temperature

$$\frac{L}{|b|} = \frac{\xi}{|b|} \ln \frac{1 + \xi/|b|}{1 - \xi/|b|}, \quad (4.4)$$

valid for $b < 0$ and $\xi/|b| < 1$ only. This remarkable relation describes the increase of the film critical temperature $T_c(L)$ upon reduction of the film thickness L . It is graphically represented in Fig. 4. Since $\xi/|b| \propto |T - T_c|^{-1/2}$, and the surface critical point of the semi-infinite system (with a single surface) lies at $T_{cs} > T_c$ such that $\xi(T_{cs})/b = -1$, relation (4.4)

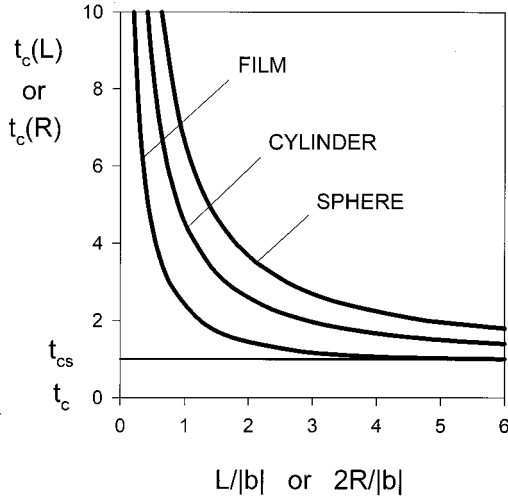


FIG. 4. Increase of the critical temperature as a function of the thickness or diameter of mesoscopic superconductors with surface enhancement. The temperature variable is $t_c(L) \equiv [T_c(L) - T_c] / [T_c(\infty) - T_c]$, where L is the film thickness, to be replaced by $2R$ for cylinders or spheres. $T_c(\infty)$ equals the surface critical temperature T_{cs} of a semi-infinite sample, and exceeds T_c . The important difference between curved and planar surfaces is the long-range (algebraic) decay of the critical-point shift for large radius.

predicts that $T_c(L) > T_{cs}$. A convenient temperature variable for our purposes is $b^2/\xi^2 = (T - T_c)/(T_{cs} - T_c)$, which we denote by t (see Fig. 4). With this notation, $t_c = 0$ and $t_{cs} = 1$, as in previous sections.

Equation (4.4) can be written in more compact form if we express the film thickness as L/ξ ,

$$\frac{\xi}{|b|} = \tanh \frac{L}{2\xi} \quad (4.5)$$

but we remark that sample size and temperature are mixed when using the variable L/ξ . We distinguish two regimes: the macroscopic regime $L \gg \xi$, and the microscopic regime $L \ll \xi$. In between is the mesoscopic range $L \approx \xi$. In the macroscopic limit (4.5) gives the critical-point shift

$$\xi/b = -1 + 2e^{-L/\xi} \quad (4.6)$$

or, using the definition $t \equiv b^2/\xi^2$,

$$t_c(L) = 1 + 4e^{-L/\xi}. \quad (4.7)$$

Clearly, for $L \rightarrow \infty$, while keeping the coherence length finite, the ratio ξ/b converges exponentially fast to -1 . This signifies that $T_c(L)$ decreases towards T_{cs} . In contrast, simple finite-size scaling ideas would suggest that $T_c(L)$ converge to the bulk T_c . This is not the case for our system, and therefore the finite-size shift in zero field is *anomalous*.

For microscopically small thicknesses ($L \ll \xi$) the increase of the critical temperature follows the power law

$$t_c(L) \approx 2|b|/L. \quad (4.8)$$

Of course, the achievement of very small thicknesses (sub-micron to nanometer range) is subject to practical limitations.

The increase of $T_c(L)$ upon reduction of the film thickness is analogous to an effect that has been uncovered in the context of twinning-plane superconductivity.⁴ Certain materials (Sn and Nb) display enhancement of superconductivity near an internal twinning plane. In a situation with closely spaced twinning planes, the enclosed slab of material experiences a transition to superconductivity at $T_c(L)$ given by the same relation as Eq. (4.4). Twinning-plane superconductivity is a special phenomenon. We would like to emphasize that the increase of $T_c(L)$ due to confinement is a more general phenomenon and occurs for thin films with surface enhancement, regardless of the precise microscopic origin of the enhancement.

Dissimilar surfaces. As a first concrete example, we consider enhancement on one surface only and assume that the other surface corresponds to a direct contact with vacuum or an insulator. We take $b_1 < 0$ and $b_2 = \infty$. In this case the increase of $T_c(L)$ still follows a law similar to Eq. (4.4) but to obtain the same transition temperature increase a further film thickness reduction by a factor of 2 is required,

$$\frac{L}{|b|} = \frac{\xi}{2|b|} \ln \frac{1 + \xi/|b|}{1 - \xi/|b|}. \quad (4.9)$$

In a second example we make the second surface unfavorable to superconductivity by introducing suppression of the wave function by assuming $b_2 > 0$ and $b_2 > |b_1|$. Physically, this corresponds to direct contact with a normal metal. The two surfaces are now in competition and the increase of $T_c(L)$ with decreasing film thickness qualitatively still behaves as in Fig. 4, but becomes progressively weaker as b_2 is decreased. The enhancement effect is lost in the antisymmetric limit $b_2 \rightarrow -b_1$.

B. Cylindrical wire

For the case of axial symmetry we adopt cylindrical coordinates and write the linearized GL equation in zero external field in the familiar Schrödinger equation form

$$-\frac{\hbar^2}{2m} \left(\frac{1}{r} \frac{\partial}{\partial r} \left(r \frac{\partial \psi}{\partial r} \right) + \frac{1}{r^2} \frac{\partial^2 \psi}{\partial \phi^2} + \frac{\partial^2 \psi}{\partial z^2} \right) = -\alpha \psi. \quad (4.10)$$

The coherence length and thus the temperature is related to the ‘‘energy’’ $-\alpha$ through $\hbar^2/2m|\alpha| = \xi^2$, with m twice the electron mass. The boundary condition on the cylinder surface, at $r=R$, reads

$$\frac{\partial \psi}{\partial r} \Big|_{r=R} = -\frac{\psi(R)}{b} \quad (4.11)$$

with $b < 0$ for surface enhancement of superconductivity.

Solutions are of the form $\psi(r, \phi, z) = f(r)e^{il\phi}e^{ikz}$. Since we are looking for the lowest ‘‘energy,’’ we can set $k=0$ and $l=0$. Indeed, for $k \neq 0$ the energy simply increases by a positive amount proportional to k^2 . Also, for $l \neq 0$, the energy is strictly greater than for $l=0$. This is due to the strict positivity of the angular momentum contribution, in combination with Ritz’ theorem

$$E_l \equiv \frac{\langle \psi_l | H | \psi_l \rangle}{\langle \psi_l | \psi_l \rangle} = \frac{\langle \psi_l | H_0 | \psi_l \rangle}{\langle \psi_l | \psi_l \rangle} + \frac{\langle \psi_l | L_z^2 / 2mr^2 | \psi_l \rangle}{\langle \psi_l | \psi_l \rangle}$$

$$> \frac{\langle \psi_l | H_0 | \psi_l \rangle}{\langle \psi_l | \psi_l \rangle} \geq \frac{\langle \psi_0 | H_0 | \psi_0 \rangle}{\langle \psi_0 | \psi_0 \rangle} \equiv E_0. \quad (4.12)$$

Here H_0 is the first term of the Hamiltonian, associated with the radial kinetic energy. The scalar product is defined on the support $r \in [0, R]$ for functions that satisfy the boundary condition (4.11). Note that this boundary condition drives the ground state energy negative, corresponding to tunneling states with negative kinetic energy. Note that the temperature for onset of superconductivity lies above T_c , since $\alpha > 0$ in the ground state.

After rescaling r by ξ , it is easily seen that the ground state eigenfunction is the modified Bessel function $I_0(r/\xi)$, which has the shape of a ‘‘hammock’’ with a smooth minimum on the cylinder axis and a maximum on the surface. Application of the boundary condition leads to the nucleation condition

$$\frac{\xi}{|b|} = \frac{I_1(R/\xi)}{I_0(R/\xi)}. \quad (4.13)$$

If we make the identification $L \equiv 2R$ we can compare this critical-point shift for the cylindrical wire with that of the thin film. This is done in Fig. 4, with again $t \equiv b^2/\xi^2$. Note that t is plotted versus $2R/|b|$ instead of $2R/\xi$. With this choice of variables it is understood that b is a *fixed* material constant, so that Fig. 4 presents a temperature versus diameter diagram.

It is obvious that the increase of T_c for cylinders is stronger than for films. This is seen dramatically in the experimentally most relevant asymptotic regime of large radius, $R \gg \xi$, for which we obtain the power law

$$\frac{\xi}{|b|} \approx 1 - \frac{\xi}{2R}. \quad (4.14)$$

This implies a slowly decaying *algebraic critical-point shift*

$$t_c(R) \approx 1 + \xi/R, \quad (4.15)$$

so that $T_c(R) - T_{cs} \propto 1/R$, in contrast with the exponential decay found for the film.

On the other hand, for small radii, $R \ll \xi$, we obtain

$$t_c(R) \approx 2|b|/R \quad (4.16)$$

which is similar to Eq. (4.8).

C. Spherical grain

Using similar arguments as for the cylinder one sees that in zero field it suffices to work with the radial wave function, which satisfies the differential equation

$$-\frac{\hbar^2}{2m} \frac{1}{r} \frac{\partial^2}{\partial r^2} (rf) = -\alpha f \quad (4.17)$$

with the same boundary condition (4.11) but now applicable to the surface of the sphere. Writing $u = rf$ and using $u(0) = 0$, we find $u(r) \propto \sinh(r/\xi)$. Application of the boundary condition then leads to the nucleation condition

$$\xi/|b| = \coth(R/\xi) - \xi/R \quad (4.18)$$

which results in an increase of $T_c(R)$ upon a reduction of $R/|b|$ shown in Fig. 4. The effect is stronger yet for spheres than for cylinders.

The asymptotic critical-point shift for large R is algebraic

$$\xi/|b| \approx 1 - \xi/R \quad (4.19)$$

implying $T_c(R) - T_{cs} \propto 1/R$ as for cylinders, but with an amplitude larger by a factor of 2. Note that the mean curvature differs from that of the cylinder by the same factor. The effect of confinement is therefore most pronounced for mesoscopic spherical grains.

Finally, in the microscopic limit $R \ll \xi$ we find

$$t_c(R) \approx 3|b|/R. \quad (4.20)$$

Recapitulating, we find that for cylinders and spheres the increase of $T_c(R)$ is *qualitatively* stronger than that of $T_c(L)$ for films, in view of the $1/R$, or ‘‘curvature’’ dependence of the critical-point shift.

D. Comparison between spherical and cubic grains

In going from a planar film to a cylindrical wire and a spherical grain the effective dimensionality of the system is reduced from 2 to 1 and 0, respectively. An alternative way of reducing the dimensionality is to go from a planar film to a rectangular rod and a cubic grain. In this case, however, the surface is not smoothly curved, but displays strong geometric singularities in the form of sharp edges and corners. In this subsection we calculate the critical-point shift for rectangular sample topology.

Consider a hypercube in n dimensions ($n = 1, 2$ or 3) of size L^n and extend the system infinitely in the remaining $3 - n$ dimensions. The choice $n = 1$ reproduces the case of the planar film, $n = 2$ the rod with square cross-section and $n = 3$ the cubic grain. Note that the effective dimensionality is $d = 3 - n$. The GL equation in zero field takes the form

$$-\frac{\hbar^2}{2m} \Delta \psi = -\alpha \psi \quad (4.21)$$

with $\alpha > 0$ since $T > T_c$. The boundary conditions on the faces of the hypercube read

$$\left. \frac{\partial \psi}{\partial x_i} \right|_{x_i=0} = \frac{\psi(x_i=0)}{b},$$

$$\left. \frac{\partial \psi}{\partial x_i} \right|_{x_i=L} = -\frac{\psi(x_i=L)}{b}, \quad (4.22)$$

where $i = 1, \dots, n$ and $b < 0$.

The technique of separation of variables leads in this case to the exact ground state, since, as we shall show, the wave function has no nodes. Thus we assume the product form

$$\psi(\{x_i\}) = \prod_{i=1}^n f_i(x_i). \quad (4.23)$$

Solutions to Eq. (4.21) are of the form

$$f_i(x_i) = A_i e^{x_i/\xi_i} + B_i e^{-x_i/\xi_i}. \quad (4.24)$$

The decay lengths ξ_i satisfy the constraint

$$\sum_{i=1}^d \xi_i^{-2} = \xi^{-2} \equiv 2m\alpha/\hbar^2. \quad (4.25)$$

Imposing the boundary conditions leads to the equations

$$\frac{L}{\xi_i} = \ln \left| \frac{1 + \xi_i/|b|}{1 - \xi_i/|b|} \right|, \quad i = 1, \dots, n \quad (4.26)$$

In order for the wave function to possess no nodes, and therefore to correspond to the exact ground state of the Schrödinger problem equivalent to our system of equations, it is necessary to consider only the solutions for which $\xi_i/|b| < 1$. Furthermore, for a given ratio $L/|b|$ this solution is nondegenerate and isotropic, so that

$$\xi_i = \xi \sqrt{d}, \quad i = 1, \dots, n. \quad (4.27)$$

The critical-point shift for $L \gg \xi$ is now given by

$$t_c(L) \approx n(1 + 2e^{-L/(\xi\sqrt{n})}). \quad (4.28)$$

The exponential decay of the shift $T_c(L) - T_c(\infty)$ turns out to be characteristic for rectangular geometry, in contrast with the power-law decay for curved surfaces. Moreover, since the condition $\xi_i/b = -1$ differs from the condition $\xi/b = -1$, the temperature of onset of superconductivity in the thermodynamic limit $L \rightarrow \infty$ depends on n in rectangular geometry. We find

$$t_c(\infty) = (T_c(\infty) - T_c)/(T_{cs} - T_c) = n, \quad (4.29)$$

with T_{cs} the surface critical temperature for a single planar surface (in a semi-infinite system).

It is a paradox that the transition temperature in the thermodynamic limit $L \rightarrow \infty$ depends on the shape of the sample. However, after some reflection it is clear that in this limit the onset of superconductivity is limited to the vicinity of the surface (for $n=1$), the vicinity of the wedge where two surfaces meet at right angles (for $n=2$) and the vicinity of the corners (for $n=3$), where superconductivity is strongly enhanced. Away from these boundaries, in the interior of the system, very little superconductivity should be expected just below $T_c(\infty)$. Therefore, from a physical point of view, the fact that $T_c(\infty) > T_c$ reflects boundary superconductivity rather than bulk superconductivity.

In the microscopic limit ($L \ll \xi$) we obtain

$$t_c(L) \approx 2n|b|/L \quad (4.30)$$

which corresponds well to the results for the curved surfaces, if, as usual, we make the identification $L = 2R$.

V. CONCLUSIONS

In this paper we have established a close analogy between capillary condensation in fluids and the transition from surface superconductivity to mesoscopic sample superconductivity. Furthermore, the interplay between capillary condensation, prewetting and wetting, has been studied in superconductors which display an interface delocalization transition. In the limit of strongly type-I superconductors a full analytic description has been given for the finite-size

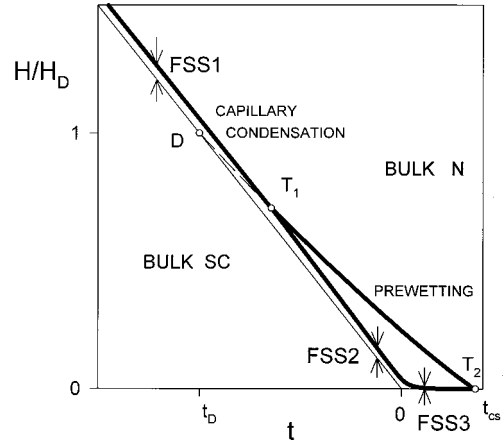


FIG. 5. Finite-size scaling (FSS) of the capillary condensation transition at $\kappa=0$ illustrated for a thick film, with $L/|b|=20$. See also Fig. 1 for comparison. The arrows FSS1 show the algebraic shift of order $1/L$ between the film transition and the bulk transition, in the partial wetting regime (no surface sheaths intervene). FSS2 indicates the similar shift in the complete wetting regime (with surface sheaths induced by the prewetting transition). For $T > T_c$ the exponentially small shift is apparent (FSS3) and clarifies how the capillary condensation line eventually converges, for large L , to a corner shape or “dog leg” consisting of the bulk coexistence line supplemented with the segment $[T_c, T_{cs}]$ on the temperature axis.

effects on the various phase transitions involved.

We have scrutinized the anomalous critical-point shift in mesoscopic samples in zero field, and the standard finite-size scaling for the transition to superconductivity in nonzero magnetic field. The critical-point shift in zero field is anomalous in the sense that $T_c(L)$ or $T_c(R)$ converges to $T_c(\infty) > T_c$ instead of T_c . Standard finite-size scaling would have predicted $T_c(\infty) = T_c$. However, in a fixed nonzero magnetic field H , no matter how small, the transition temperature in the limit $L \rightarrow \infty$ (or $R \rightarrow \infty$) converges to the temperature associated with the bulk critical field $H_c = H$. In other words, in nonzero field the bulk two-phase coexistence line is fully restored in the macroscopic or “thermodynamic” limit.

The anomaly is thus confined to the temperature segment $[T_c, T_{cs}]$ in vanishing field. This segment becomes part of the two-phase coexistence line in the limit of large thickness or diameter of the sample. As a result, the capillary condensation line displays a corner or bend in the vicinity of $(T = T_c, H = 0)$. How this corner develops can be seen in Fig. 5, which shows the phase diagram for $L/|b|=20$. Comparing this with Fig. 1, which corresponds to $L/|b|=8$ we notice that the capillary condensation line approaches the bulk coexistence line in nonzero field, but the supercritical temperature segment remains part of the capillary condensation line.

We have indicated by FSS1 the finite-size shift of the capillary condensation transition in the partial wetting regime. Likewise, FSS2 refers to the finite-size shift in the complete wetting regime, and FSS3 marks the shift in the supercritical region. These shifts obey the analytical laws derived in Sec. III. For this large value of $L/|b|$ the critical-point shift in zero field is so (exponentially) small that $T_c(L)$ practically coincides with T_{cs} .

The significance of the zero-field critical temperature in the macroscopic limit $T_c(\infty)$ must be considered with care.

For planar, cylindrical and spherical geometry, $T_c(\infty) = T_{cs}$. This implies that for asymptotically flat surfaces (with vanishing curvature everywhere) superconductivity starts near the surface. For macroscopic cubes, however, superconductivity can start at higher T because it nucleates first in wedges and corners. This is why, for square rods and cubes, $T_c(\infty)$ is progressively increased. This apparent increase of T_c in the macroscopic limit disappears when the sharp edges are fully rounded. In the mesoscopic and microscopic regimes smoothing of corners or other asperities is irrelevant, since shape details are then small relative to the scale of ξ and cannot be “resolved.” The critical temperature is then independent of the details of the shape of the sample.

From a more practical point of view our most noteworthy result is the significant increase of $T_c(R)$ for mesoscopic cylindrical or spherical superconductors with surface enhancement. The main asymptotic relation between $T_c(R)$ and the sample radius can be summarized in the form, to leading order in $1/R$,

$$t \approx 1 + 2c\xi, \quad (5.1)$$

where $t \equiv (b/\xi)^2 = [T_c(R) - T_c]/(T_{cs} - T_c)$, and $c \equiv (1/R_1 + 1/R_2)/2$ is the mean curvature. For cylinders, $c = 1/2R$. For spheres, $c = 1/R$.

We illustrate the theoretically predicted increase of T_c by means of a numerical example based on the (old) results of Fink and Joiner³ for a surface-enhanced $\text{In}_{0.993}\text{Bi}_{0.007}$ foil, with $T_c \approx 3.5$ K, and $\kappa \approx 0.37$. After cold working of the sample surface the critical temperature increased to $T_{cs} = T_c + 0.02$ K. An order of magnitude estimate suffices, so we take a typical value for the coherence length amplitude, $\xi_0 \approx 1000$ Å and obtain $\xi(T_{cs}) = \xi_0(T_{cs}/T_c - 1)^{-1/2} \approx 1.3$ μm. Since $b = -\xi(T_{cs})$ we obtain that $|b|$ is of the order of a micron.

This estimate allows us to predict the further increase of T_c due to confinement. For example, for a thin film of thickness $L = 10$ μm of the same alloy the predicted $T_c(L)$ on the basis of Eq. (4.4) is still $T_c + 0.02$ K. The confinement effect is imperceptible for this thickness. Reducing the thickness further to $L = 1$ μm we obtain $T_c(L) = T_c + 0.05$ K and for $L = 0.1$ μm we find $T_c(L) = T_c + 0.41$ K. Now, changing the geometry from planar to cylindrical or spherical the increase of T_c is more striking. For example, for a spherical grain of diameter 10 μm of the same material, Eq. (4.15) predicts $T_c(R) = T_c + 0.03$ K. For $2R = 1$ μm we obtain $T_c(R) = T_c + 0.13$ K, and for $2R = 0.1$ μm we get $T_c(R) = T_c + 1.21$ K = 4.71 K.

We would like to stress that cold working of the sample surface is only one of the possible surface treatments that can lead to surface enhancement of the superconducting order parameter. In modern experiments deposition of a thin layer (of thickness less than the coherence length) can be performed in a clean, controlled and reproducible way. This layer affects the boundary condition, and measurement of the critical temperature in zero field is sufficient to establish the sign and, for $b < 0$, also the magnitude of the surface extrapolation length b .

Further, our results for zero magnetic field are independent of the GL parameter κ and thus apply to type-I and

type-II superconductors alike. In our opinion the results concerning the increase of T_c are possibly also relevant for surface-enhanced high- T_c superconductors. The reason for this belief is that in at least two experiments surface enhancement was found in high- T_c materials. Fang *et al.* measured an increase of T_c of several degrees K in macroscopic YBaCuO samples with twinning planes,¹⁸ and Schwartzkopf *et al.* in HoBaCuO.¹⁹ Abrikosov and Buzdin²⁰ invoked the GL theory with the same boundary condition $b < 0$, to describe this phenomenon.

In a future publication we intend to report on calculations of global H - T phase diagrams for $\kappa > 0$. In addition to the features we have discussed in this paper, second-order transition lines and tricritical points appear. Also, the film vortex phase becomes stable in a small region of the phase diagram, and gains importance as κ is increased.

ACKNOWLEDGMENTS

We thank François Peeters and Todor Mishonov for stimulating discussions, and Ralf Blossey and Harvey Dobbs for comments on the manuscript. This research was supported by the Flemish FWO Project No. G.0277.97 and by the Inter-University Attraction Poles and the Concerted Action Program.

APPENDIX: CAPILLARY CONDENSATION APPROACHING COMPLETE WETTING

In this appendix we are concerned with the derivation of Eq. (3.8). The starting point is the condition for capillary condensation $\gamma_{PW} = \gamma_{cap}$. This is worked out as follows:

$$\gamma_{PW} - \gamma_{cap} = 2\gamma_{SC,N} - (H_R^2 - 1/2)(L - 2l)/\xi + \delta\gamma_{PW} - \delta\gamma_{cap}. \quad (A1)$$

The term $\delta\gamma_{PW}$ represents the free energy of two constrained wetting layers minus that of two equilibrium wetting layers. If we adopt the notation

$$J(\psi; A, B) = \frac{A - \psi^4/2}{\sqrt{-\psi^2 + \psi^4/2 + B}} \quad (A2)$$

we obtain

$$\delta\gamma_{PW} = 2 \int_0^{\psi_{PW}^{(0)}} d\psi J(\psi; 1/2, H_R^2) - 2 \int_0^{\psi^{(0)}} d\psi J(\psi; 1/2, 1/2). \quad (A3)$$

The fact that the argument A of the function J equals $1/2$ in both terms signifies that H_R is set equal to $H_{R,c}$. The constraint is imposed by setting the argument B equal to $H_R^2 > 1/2$ in the first term only, so that the constrained layer has the same thickness and profile as an equilibrium layer in a field H_R . For more details on the physics of constrained surface sheaths, we refer to Ref. 9.

The term $\delta\gamma_{cap}$ represents the free energy of the capillary condensed state minus $2\gamma_{W,SC}$,

$$\delta\gamma_{\text{cap}} = 2 \int_{\psi_m}^{\psi_{\text{cap}}(0)} d\psi J(\psi; 1/2, C) - 2 \int_1^{\psi(0)} d\psi J(\psi; 1/2, 1/2), \quad (\text{A4})$$

where $C = C(L)$ is the ‘‘constant’’ in the first integral for superconducting film states (2.3).

We now examine the calculation of these terms, and begin with $\delta\gamma_{\text{PW}}$. We define $\epsilon = H_R^2 - 1/2$ and consider an expansion to first order in ϵ . The first contribution comes from the ϵ -dependent upper limit of the integral. Explicitly,

$$\psi_{\text{PW}}(0)^2 = 1 + (\xi/b)^2 + \sqrt{[1 + (\xi/b)^2]^2 - (1 + 2\epsilon)}. \quad (\text{A5})$$

For $\epsilon \rightarrow 0$, $\psi_{\text{PW}}(0)$ reduces to $\psi(0)$. The second contribution comes from the ϵ dependence of the integrand $J(\psi; 1/2, H_R^2)$. After some elementary algebra, we find to first order

$$\begin{aligned} \frac{\delta\gamma_{\text{PW}}}{\sqrt{2}\epsilon} &= \frac{\psi(0)^2 + 1}{2\psi(0)[\psi(0)^2 - 1 - (\xi/b)^2]} \\ &+ \lim_{\epsilon \rightarrow 0} \left(\int_1^{\psi(0)} - \int_0^1 \right) d\psi \frac{1 + \psi^2}{(1 - \psi^2)^2 + \epsilon}. \end{aligned} \quad (\text{A6})$$

The evaluation of the limit must be done carefully. We have separated the integrand into a symmetric and an antisymmetric part (with respect to $\psi = 1$). The symmetric part, which contains the dominant singularity proportional to $1/(\psi - 1)^2$, is largely canceled by subtracting the integrals. In the part that remains one may safely set $\epsilon = 0$ and the result is the contribution, with $x = \psi - 1$,

$$\delta_{\text{sym}} = - \int_{\psi(0)-1}^1 dx \frac{8 - 2x^2 + x^4}{x^2(4 - x^2)^2} \quad (\text{A7})$$

which is simple to evaluate. In the antisymmetric part, however, one may not exchange the limit $\epsilon \rightarrow 0$ with the integration. One must calculate

$$\begin{aligned} \delta_{\text{antisym}} &= \lim_{\epsilon \rightarrow 0} \left(\int_0^1 + \int_0^{\psi(0)-1} \right) \\ &\times dx \frac{2\epsilon x - 2x^5}{\epsilon^2 + 8\epsilon x^2 + 2\epsilon x^4 + 16x^4 - 8x^6 + x^8}. \end{aligned} \quad (\text{A8})$$

This leads to two contributions, associated with the two terms in the numerator of the integrand. The result is, with $z = x^2/\epsilon$,

$$\delta_{\text{antisym}} = \int_0^\infty dz \frac{2}{(1 + 4z)^2} - \left(\int_0^1 + \int_0^{\psi(0)-1} \right) dx \frac{2x}{(4 - x^2)^2} \quad (\text{A9})$$

which is elementary to evaluate.

The final result is

$$\delta\gamma_{\text{PW}} = \sqrt{2}\epsilon + o(\epsilon). \quad (\text{A10})$$

The correction $o(\epsilon)$ goes to zero faster than ϵ , in the manner $a\epsilon^2 \log(1/\epsilon)$, according to numerical computations. For example, for $\xi/b = -1$ we obtain $a \approx 0.26$. It is interesting to note that the leading-order term is independent of $\psi(0)$, and thus independent of the ‘‘temperature’’ variable ξ/b .

We now turn to the evaluation of $\delta\gamma_{\text{cap}}$. As a first step we examine the dependence $C(L)$ for capillary condensation states more closely. For this it suffices to study the leading terms in L/ξ for $C \rightarrow 1/2$ from below. Using Eq. (2.4), together with the relations $\psi_m = [1 + (1 - 2C)^{1/2}]^{1/2}$ and $\psi_{\text{cap}}(0)^2 = 1 + (\xi/b)^2 + \{[1 + (\xi/b)^2]^2 - 2C\}^{1/2}$, we obtain after some algebra,

$$\frac{L}{\xi} = \frac{1}{\sqrt{2}} \ln \frac{1}{1/2 - C} + D + o(1), \quad (\text{A11})$$

where $o(1)$ denotes terms that vanish for $C \rightarrow 1/2$. We verified numerically that the constant D is typically of order unity and depends on ξ/b . This result implies the (expected) exponential decay of $C(L)$ for large L ,

$$(1/2 - C) \propto e^{-\sqrt{2}L/\xi}. \quad (\text{A12})$$

In a second step we find, using numerical computation, that for C approaching $1/2$,

$$\delta\gamma_{\text{cap}} \approx - \frac{1}{\sqrt{2}} \left(\frac{1}{2} - C \right) \quad (\text{A13})$$

so that the finite-size correction for the surface free energy of the capillary condensed profile decays exponentially rapidly with the thickness of the film, in view of Eq. (A12). The fact that $\delta\gamma_{\text{cap}}$ is negative expresses the lowering of the free energy of the superconducting film by confinement. This is a manifestation of the fairly general observation that ‘‘like’’ surfaces attract each other.²¹ In contrast, $\delta\gamma_{\text{PW}} > 0$, reflecting the repulsion between the SC/N interface and the surface.

¹For a review, see, e.g., V. L. Ginzburg, Phys. Usp. **40**, 407 (1997).

²D. Saint-James and P. G. de Gennes, Phys. Lett. **7**, 306 (1963)

³H. J. Fink and W. C. H. Joiner, Phys. Rev. Lett. **23**, 120 (1969).

⁴I. N. Khlyustikov and A. I. Buzdin, Adv. Phys. **36**, 271 (1987).

For the theory of enhanced superconductivity at planar defects, see also N. B. Ivanov and T. M. Mishonov, Phys. Status Solidi B **142**, K49 (1987).

⁵J. O. Indekeu and J. M. J. van Leeuwen, Phys. Rev. Lett. **75**, 1618 (1995); Physica C **251**, 290 (1995).

⁶R. Evans, J. Phys.: Condens. Matter **2**, 8989 (1990).

⁷V. V. Moshchalkov, L. Gielen, C. Strunk, R. Jonckheere, X. Qiu, C. Van Haesendonck, and Y. Bruynseraede, Nature (London) **373**, 319 (1995).

⁸P. S. Deo, V. A. Schweigert, F. M. Peeters, and A. K. Geim, Phys. Rev. Lett. **79**, 4653 (1997); V. A. Schweigert and F. M.

- Peeters, Phys. Rev. B **60**, 3084 (1999).
- ⁹R. Blossey and J. O. Indekeu, Phys. Rev. B **53**, 8599 (1996).
- ¹⁰C. J. Boulter and J. O. Indekeu, Phys. Rev. B **54**, 12 407 (1996).
- ¹¹J. M. J. van Leeuwen and E. H. Hauge, J. Stat. Phys. **87**, 1335 (1997).
- ¹²A. Winter, Heterog. Chem. Rev. **2**, 269 (1995).
- ¹³See, e.g., M. E. Fisher, J. Chem. Soc., Faraday Trans. 2 **82**, 1569 (1986).
- ¹⁴For a review, see S. Dietrich, in *Phase Transitions and Critical Phenomena*, edited by C. Domb and J. L. Lebowitz (Academic, London, 1988), Vol. 12, p. 1.
- ¹⁵See, e.g., M. Krech, *The Casimir Effect in Critical Systems* (World Scientific, Singapore, 1994).
- ¹⁶M. Kardar and R. Golestanian, Rev. Mod. Phys. (Colloq.) **71**, 1233 (1999).
- ¹⁷E. Montevecchi and J. O. Indekeu (unpublished).
- ¹⁸M. M. Fang, V. K. Kogan, D. K. Finnemore, J. R. Clem, L. S. Chumbley, and D. E. Farrell, Phys. Rev. B **37**, R2334 (1988).
- ¹⁹L. A. Schwartzkopf, M. M. Fang, L. S. Chumbley, and D. K. Finnemore, Physica C **153-155**, 1463 (1988).
- ²⁰A. A. Abrikosov and A. I. Buzdin, Pis'ma Zh. Eksp. Teor. Fiz. **47**, 204 (1988) [JETP Lett. **47**, 247 (1988)].
- ²¹M. P. Nightingale and J. O. Indekeu, Phys. Rev. Lett. **54**, 1824 (1985); J. O. Indekeu, M. P. Nightingale, and W. V. Wang, Phys. Rev. B **34**, 330 (1986).